Journal of Solid Mechanics Vol. 13, No. 2 (2021) pp. 114-133
DOI: 10.22034/jsm.2020.1883837.1520

# On The Free Vibration of Doubly Clamped Single-Walled Coiled Carbon Nanotubes: A Novel Size Dependent Continuum Model

F. Darvishi, O. Rahmani*

*Department of Mechanical Engineering, University of Zanjan, Zanjan, Iran*

Received 11 February 2021; accepted 28 March 2021

**ABSTRACT**

In this paper, the size dependent vibration behavior of doubly clamped single-walled coiled carbon nanotubes (CCNTs) is investigated using nonlocal helical beam model. This model is based on Washizu's beam theory so that all displacement components of CCNT in the equations of motion are defined at the centroidal principal axis and transverse shear deformations are considered. After deriving the nonlocal free vibration equations, they are solved by the generalized differential quadrature method (GDQM). Then, the natural frequencies and corresponding mode shapes are determined for the clamped-clamped boundary conditions (BCs). After that, a parametric study on the effect of different parameters, including the helix cylinder to the tube diameters ratio $(D/d)$, the number of pitches, the helix pitch angle, and the nonlocal parameter on the natural frequencies is conducted. It is worth noting that the results of the proposed method would be useful in the practical applications of CCNTs such as using in nanoelectromechanical systems.



**Keywords :** Free vibration; Coiled carbon nanotubs; Helical spring model; Nonlocal elasticity theory; Differential quadrature method.

## 1 INTRODUCTION

CARBON nanotubes (CNTs) are one of the carbon morphologies, which discovered by Ijima in 1991 [1]. Existence different arrangements of non-hexagonal rings such as the pentagons and heptagons in the hexagonal network of the CNTs induce positive and negative curvatures, which can bend and twist the CNTs into a variety of different shapes, as toroidal carbon nanotubes (TCNTs) and coiled carbon nanotubes (CCNTs) [2]. The single-walled coiled carbon nanotubes (CCNTs) were proposed theoretically by Ihara et al. in 1993 [3]. The first experimental observation of single-walled CCNTs were performed using scanning tunneling microscopy (STM) by Biró et al. in 2000 [4]. In Fig. 1, the scanning electron microscopy (SEM) image of a vertically grown CCNT and formation of CCNTs during the chemical vapor deposition (CVD) synthesis process is shown [5].The CCNTs have major potential applications in various fields due to their unique spiral structures and the extraordinary physical

*Corresponding author. Tel.: +98 9122414371.
*E-mail address: omid.rahmani@znu.ac.ir* (O. Rahmani)

characteristics. One important application for CCNTs is to act as sensors. The CCNTs with attached electrodes can be used as self-sensing mechanical resonators, so that they are able to detect fundamental resonances ranging from 100 to 400 *MHz* The self-sensing CCNTs sensors are sensitive to mass change and well suited for measuring small forces and masses in the femtogram range [6]. Also, the CCNTs can be applied as high-resolution force sensors in conjunction with visual displacement measurement as well as electromechanical sensors [7].

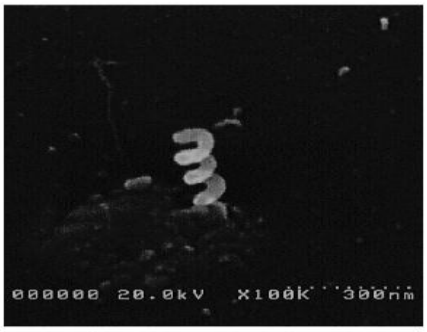


**Fig.1**
SEM image of a vertically grown coiled carbon nanotubes [5].

Another application of CCNTs is the usage in reinforced high-strain composites due to the higher toughness compared to the carbon fibers. Also, they can be anchored better in their embedding matrix than CNTs [8]. Moreover, CCNTs can be used in nanoelectromechanical systems (NEMS) [9] and electromechanical devices such as non-volatile random access memory (RAM), actuators, gears and receivers [5]. In addition, the CCNTs can be used as molecular Nano solenoids in nano-switches and electromagnetic nano-transformers [10]. It is necessary to study the mechanical properties and vibrational behavior of the CCNTs for better understanding of their applications. Since experimental studies at nanoscale size is quite expensive and time consuming, theoretical methods are preferred. Theoretical methods to study the nanostructures are categorized into atomistic modeling and non-classical continuum mechanics. Among the atomistic modeling methods, classical molecular dynamics (MD), tight-binding (TB) and density functional theory (DFT) can be mentioned, which need high computational costs. Hence, the use of non-classical continuum theories like nonlocal elasticity theory, strain gradient theory and couple stress theory, which are developed to consider the size effect, can play a significant role in the study of nanostructures [11]. Several theoretical studies were carried out to assessment the mechanical properties of single-walled CCNTs and CCNT-reinforced nanocomposites. Fonseca et al. [12] using the Kirchhoff rod model, derived a series of expressions to obtain Young's modulus and Poisson's ratio of the CCNTs. Liu et al [13] employing DFT and TB methods calculated the Young's modulus and elastic constant of a series of CCNTs built from the armchair single-walled CNTs and predicted superelastic behavior of the CCNTs. Ghaderi and Hajiesmaili [14] using the MD-based finite element method determined fracture strain, fracture load, and energy storage density of the CCNTs. Wang et al. [15] via the MD simulations and the second generation of the reactive empirical bond-order (REBO) potential and Lennard-Jones (LJ) potential investigated the mechanical properties of a coiled carbon nanotube (CCNT) under compression, tension, re-compression, re-tension and pullout from a polyethylene (PE) matrix. They obtained spring constants, yielding strains and pullout force of the CCNT. Wu et al [16] using the MD simulations and with the adaptive intermolecular reactive empirical bond-order (AIREBO) potential and obtained stiffness and gravimetric toughness for them. Khani et al. [17] using new representative volume element (RVE) generation method based finite element and evaluated the effect of volume fraction, orientation geometry of the CCNTs on the elastic moduli of the nanocomposites. Kianfar et al. [18] presented three-dimensional finite element modeling of the CCNT-reinforced polymer nanocomposites and generated representative volume elements to determine the mechanical behavior in elastic and plastic zones. They studied the effects of different volume fractions, geometrical parameters and orientations of the CCNTs on the elastic characteristics of the nanocomposites. Yarali et al. [19] numerically investigated the thermomechanical properties of the coiled carbon nanotube reinforced shape memory polymer nanocomposites (SMP) under large deformations. They employed a thermo-visco-hyperelastic constitutive model for SMP and introduced a cubic RVE using Monte Carlo algorithm. Then, the effect of inclusion's geometry, volume fraction, as well as their distribution on the thermomechanical properties of SMP/CCNT composite in two stress- and shape recovery processes in different heating rates and pre-strains is studied using finite element (FE) technique. So far, two theoretical studies were carried out to investigate the free vibration behavior of the CCNTs. Fakhrabadi et al. [20], studied the vibration behavior of the single-walled CCNTs using molecular mechanics based finite element method (MMFEM) and 3D elastic beam elements. They determined the natural frequencies and mode shapes of CCNTs with different geometries and boundary conditions. Rahmani and Darvishi [21], investigated the

free longitudinal vibration of single-walled CCNTs via MD simulation method and with the reactive empirical bond order (REBO) potential. They evaluated the influence of different parameters, including diameter of tubes, number of pitches and various boundary conditions on the fundamental frequencies. However, several studies have been conducted to investigate the free vibration behavior of straight and curved carbon nanotubes. For example, Arash et al. [22] studied the potential of CNTs as nano sensors in detection of genes through a vibration analysis with molecular dynamics simulation. Different genes are detected by identifying a differentiable sensitivity index that is defined to be the shifts of the resonant frequency of the CNT. Gajbhiye and Singh [23] studied the vibration characteristics of open- and capped-end armchair and zigzag single-walled CNTs using atomistic finite element method (AFEM). The natural frequencies are calculated for clamped-free and clamped-clamped boundary conditions. Ali-Akbari and Firouz-Abadi [24] studied the nonlinear vibration of single-walled CNTs embedded in a Kelvin-Voigt foundation. The CNT is considered as a simply-supported elastic Euler-Bernoulli beam with von-Kármán type geometrical nonlinearity. The governing equation of motion is derived based on the Hamilton's principle and the nonlocal elasticity theory. Then, the equation of motion is solved using the Galerkin method and an asymptotic perturbation method called Krylov-Bogolubov-Mitropolskij (KBM) method. The effects of amplitude, residual stresses, and viscoelastic foundation are discussed. Farokhi et al. [25] developed a new size-dependent nonlinear model for the analysis of the behaviour of carbon nanotube-based resonators using modified couple stress theory. The nonlinear partial differential equations of motion of the system are discretized by means of the Galerkin technique and the nonlinear resonant behavior is examined via the pseudo-arclength continuation technique. Hussain and Naeem [26] examined free vibrations of single-walled CNTs using wave propagation approach (WPA) and Flügge's shell model. They obtained the vibration frequency spectra and evaluated influence different boundary conditions and various physical parameters e.g., length and thickness-to-radius ratio on the natural frequencies. Tadi Beni et al. [27] using the couple stress theory provided a new model for vibrating behavior of anisotropic carbon nanotubes. The motion equations are solved using the analytical Navier method and the effect of different parameters, particularly the anisotropic effect are investigated on the carbon nanotube natural frequency.

Jiang et al. [28] investigated the vibrational behavior of single-walled CNTs bridged on a silicon channel using a three-segment Timoshenko beam model and a one-segment Timoshenko beam model together with molecular dynamics (MD) simulation. Explicit formulas are derived for the van der Waals (vdW) interaction coefficients between the SWCNTs and silicon substrates. The boundary elastic constants of the SWCNTs bridged on the silicon channel are obtained by fitting the bending curve of CNTs subjected to a static uniformly distributed lateral load simulated via the MD method. Shahabodini et al. [29] adopted the variational differential quadrature (VDQ) method for the multiscale analysis of vibrations of single-walled CNTs. They modeled CNT by a hyperelastic membrane whose kinematics is described using the higher-order Cauchy-Born rule. The effects different geometrical parameters, boundary conditions and chiralities are evaluated on the frequencies and mode shapes of CNTs. Chwal [30] analyzed the eigenfrequencies of single-walled CNTs using the nonlocal elasticity theory. The nonlocal parameter is determined for single-walled carbon nanotubes based on the finite element approximation in modeling the dynamic behavior instead of commonly used MD simulations. The effects of the length-to-diameter ratio L/D, nonlocal parameter, the influence of boundary conditions are investigated on eigenfrequencies of the CNTs. Eltaher et al. [31] investigated dynamical behaviors of perfect and defected fixed-fixed single-walled CNTs. Energy-equivalent model is implemented to find a relationship between the energy stored in atomic chemical bonding and potential energy of mechanical beam structure. The bonding between each two atoms is modeled by 3D beam element with circular cross section. The effects of vacancy are evaluated on activation and deactivation of vibration modes, fundamental frequencies, and modal participation factors of CNTs.

Majeed et al. [32] investigated vibration analysis of single-walled CNTs based on Love's thin shell theory and the wave propagation approach. The CNTs are taken into account under the influence of Winkler and Pasternak foundations. The vibrational natural frequencies of CNTs is obtained with various boundary conditions and the axial modal dependence is measured by the complex exponential functions implicating the axial modal numbers. Hussain and Naeem [33] presented formulation of Love's shell theory for single-wall carbon nanotubes (SWCNTs) using Galerkin's method. They performed vibrational analysis to investigate the effect of different mode and in-plane rigidity with clamped-clamped and clamped-free boundary conditions. Moreover, the influence of mass density per unit lateral area on the same structure is also developed. Hayati et al. [34] analyzed the free vibration behavior of a single-walled curved CNT under twist-bending couple using nonlocal theory. They solved differential equations using Navier analytical method for the simply supported boundary condition and evaluated the effect of nonlocal parameter, the curved nanotube's opening angel on the natural frequencies. Hitherto, the continuum mechanics methods have not been implemented for studying the free vibration behavior of CCNTs. Whereas, for macro-scale helical beams and springs, the formulations are presented based on beams theories such as Timoshenko beam theory and Washizu's beam theory. Wittrick [36] investigated the wave propagation on the semi-infinite springs. He

derived a set of twelve linear coupled partial differential equations for a uniform helical spring based on the Timoshenko beam theory. Thereinafter, researchers generalized the Wittrick's equations for studying the vibrational behavior of helical beams and springs, and solved the governing equations by various numerical methods such as the finite element method (FEM), the transfer matrix method (TTM), dynamic stiffness method and pseudospectral method. For example Mottershead [37] computed the natural frequencies from FEM and compared the obtained results with the results of his experimental study. Pearson [38] analyzed the free vibrations of compressed cylindrical helical springs using TMM proposed by Yildirim [39]. He evaluated the effect of boundary conditions, helix pitches angle and number of pitches on natural frequencies. In another research, Yildirim [40] investigated the free vibration of cylindrical helical springs under combined compression and torsion. Furthermore, Yildirim [41] studied the free vibration of helical springs under axial static load based on the theory of spatially curved bars and used the numerical solution method that previously had offered. Lee and Thompson [42] used the dynamic stiffness method to calculate the natural frequencies of helical springs and compared the obtained results with those of TMM and FEM. Lee [43], used the pseudo spectral method to determine the natural frequencies and corresponding mode shapes of cylindrical helical springs. He approximated the displacements and rotations by expanding the series of Chebyshev polynomials and collocated the governing equations. Then, natural frequencies and mode shapes were determined with different fixed-fixed, free-free, fixed-free and hinged-hinged boundary conditions. In an analytical study, Yu et al. [44] investigated the free vibration of naturally curved and twisted beams using Washizu's beam model [45]. They obtained explicit analytical expressions for the vibrating mode shapes under clamped-clamped boundary conditions using the symbolic computing package of Mathematica; furthermore a simple automated Muller root search method was used to determine the natural frequencies.

The main purpose of this paper is to provide an analytical formulations for studying the free vibration behvior of the singel-walled CCNTs. In this regard, a continuum model is proposed based on the nonlocal form of Washizu's beam theory. The nonlocal governing equations are derived from Hamilton's principle and solved via the generalized differential quadrature method (GDQM). The natural frequencies and the corresponding mode shapes for CCNTs are determined under the clamped-clamped boundary conditions. Finally, the effect of different parameters such as the geometric and nonlocal parameters on the natural frequencies of CCNTs are evaluated and the results are provided.

## 2 THE NONLOCAL HELICAL BEAM MODEL FOR THE CCNTs

In this section, first the Washizu's beam model is presented for helical beams and springs. Then, nonlocal governing equations are derived for CCNTs via this model and the nonlocal elasticity theory along with Hamilton's principle.

### *2.1 Washizu's beam model*

In 1964, a theory was presented by Washizu to study the naturally curved and twisted beams subjected to combined loads [45]. The relations for these beams in the curvilinear coordinate system was obtained with the aid of Frenet-Seret formulae [45] under the following assumptions:

1) The curvature of the beam is assumed to be moderate.
2) The displacement field of the beam is assumed to consist of stretching, bending and torsion deformations and non-classical effects.
3) The in-plane stress components, $\sigma_\xi$, $\sigma_\eta$ and $\tau_{\xi\eta}$, are assumed to be very small compared to the remaining components.

According to Fig. 2, the origin of the curvilinear coordinate system $(s,\xi,\eta)$, with corresponding unit vectors of $\boldsymbol{t}$, $\boldsymbol{i}_\xi$ and $\boldsymbol{i}_\eta$, is in coincidence with the cross-section center of a helical beam [44]. $s$ is arc length along the curve.

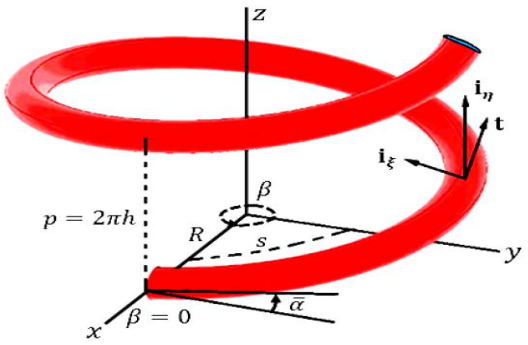


**Fig.2**
Geometry of the helical beam in the curvilinear coordinate system $(s,\xi,\eta)$.

The parametric relationships of the helical beam are [44]:

$$h = R\tan\bar{\alpha}, \qquad p = 2\pi h, \qquad C = (R^2 + h^2)^{1/2}, \qquad k_s = \frac{h}{C^2} = \frac{\sin\bar{\alpha}\cos\bar{\alpha}}{R}$$
$$k_\xi = 0, \qquad k_\eta = \frac{R}{C^2} = \frac{\cos^2\bar{\alpha}}{R} \tag{1}$$

where $h$ is the pitch for unit angle of the helix, $p$ is the pitch of the helix, $R$ is the centerline radius of the helix, $\bar{\alpha}$ is the pitch angle and $\beta$ is polar angle of the helix. $k_\eta$ and $k_s$ are the curvature and torsion of the helix, respectively.

According to the second assumption, the displacement vector $\boldsymbol{u}(s,\xi,\eta)$ is expressed as follows [45]:

$$\begin{aligned}
&\boldsymbol{u}(s,\xi,\eta) = W\boldsymbol{t} + U\boldsymbol{i}_\xi + V\boldsymbol{i}_\eta \\
&W = u_s(s) + \eta\phi_\xi(s) - \xi\phi_\eta(s) + \alpha(s)\chi(\xi,\eta) \\
&U = u_\xi(s) - \eta\phi_s(s) \\
&V = u_\eta(s) + \xi\phi_s(s)
\end{aligned} \tag{2}$$

The displacement vector is a linear function of displacement components. The deformation degrees of freedom is restricted to seven functions of $s$; three translational functions $u_s(s), u_\xi(s), u_\eta(s)$ and three rotational functions $\phi_s(s), \phi_\xi(s), \phi_\eta(s)$ along with the generalized warping coordinate $\alpha(s)$ [45].

The non-classical influences relevant to the beam are those due to the transverse shear deformations and torsion related warping [44]. The $\chi(\xi,\eta)$ is the warping function of Saint-Venant's torsion in a cylindrical shaft with the same cross-section as the considered beam [46]. In this study, since the cross-section of the CCNTs is circular, the $\chi(\xi,\eta)$ function is equal to zero. The strain-displacement relations are obtained as follows [45]:

$$\begin{aligned}
&e_{ss} = \varepsilon_s + \eta\omega_\xi - \xi\omega_\eta \\
&2e_{s\xi} = \varepsilon_\xi - \eta\omega_s \\
&2e_{s\eta} = \varepsilon_\eta + \xi\omega_s \\
&e_{\xi\xi} = e_{\eta\eta} = e_{\xi\eta} = 0
\end{aligned} \tag{3}$$

where $e_{ss}, e_{s\xi}$ and $e_{s\eta}$ are the axial and shear strain components, respectively. Also $\varepsilon_s, \varepsilon_\xi, \varepsilon_\eta, \omega_s, \omega_\xi$ and $\omega_\eta$ are generalized strains written by:

$$\begin{aligned}
&\varepsilon_s = u_s' - k_\eta u_\xi + k_\xi u_\eta \\
&\varepsilon_\xi = u_\xi' + k_\eta u_s - k_s u_\eta - \phi_\eta \\
&\varepsilon_\eta = u_\eta' - k_\xi u_s + k_s u_\xi + \phi_\xi
\end{aligned} \tag{4}$$

$$\omega_s = \phi_s' - k_\eta \phi_\xi + k_\xi \phi_\eta$$
$$\omega_\xi = \phi_\xi' + k_\eta \phi_s - k_s \phi_\eta$$
$$\omega_\eta = \phi_\eta' - k_\xi \phi_s + k_s \phi_\xi$$

where prime superscript denotes the derivative with respect to $s$ .

For the homogeneous and isotropic beams, the constitutive relationships are as follows [44]:

$$\sigma_s = E\, e_{ss} \quad ; \quad \tau_{s\xi} = 2G_\xi G\, e_{s\xi} \quad ; \quad \tau_{s\eta} = 2G_\eta G\, e_{s\eta} \tag{5}$$

where $E$ and $G$ are the Young's modulus and shear modulus of the material, respectively. The $G_\xi$ and $G_\eta$ are shape factors that are dependent on the beam sections [47]. Also, according to the third assumption, the stress components of $\sigma_\xi, \sigma_\eta$ and $\tau_{\xi\eta}$ are assumed to be very small, therefore we have:

$$\sigma_\xi = \sigma_\eta = \tau_{\xi\eta} = 0 \tag{6}$$

*2.2 Nonlocal governing equations of the CCNTs*

According to Eringen's nonlocal theory, stress at a reference point $\mathbf{x}$ in a body depend not only on the strains at that point $\mathbf{x}$, but also on the strains at all other points $\mathbf{x}'$ of the body [48]. Thus, Eringen presented the nonlocal constitutive relation, by Eq. (7), which is the spatial integral of weighted averages of strain tensors contribution of all points in to the stress tensor at a given point [11].

$$\boldsymbol{\sigma}(\mathbf{x}) = \int_\Omega \alpha(|\mathbf{x}' - \mathbf{x}|, \tau)\, \boldsymbol{t}(\mathbf{x}')\, \mathrm{d}\Omega(\mathbf{x}') \tag{7}$$

where $\Omega$ is volume of body, $\boldsymbol{\sigma}(\mathbf{x})$ and $\boldsymbol{t}(\mathbf{x})$ are nonlocal stress tensor and the local stress tensor in point $\mathbf{x}$, respectively. The stress tensor of $\boldsymbol{t}(\mathbf{x})$ is related to linear strain tensor of $\boldsymbol{\varepsilon}(\mathbf{x})$ by Hooke's law as follows:

$$\boldsymbol{t}(\mathbf{x}) = C(\mathbf{x}) : \boldsymbol{\varepsilon}(\mathbf{x}) \tag{8}$$

Here $C$ is the fourth order elasticity tensor and ':' denotes the double dot product. In Eq.(7), nonlocal modulus, $\alpha(|\mathbf{x}' - \mathbf{x}|, \tau)$, is an attenuation function, which can be determined experimentally or by fitting the dispersion curves of plane waves with those of atomic lattice dynamics [48]. $|\mathbf{x}' - \mathbf{x}|$ denotes the Euclidean distance and $\tau$ is a material constant given as:

$$\tau = \frac{e_0 a}{l} \quad ; \quad \mu = e_0 a \tag{9}$$

In which, $\tau$ depends on a characteristic length ratio $a/l$, where $a$ is an internal characteristic length (such as lattice parameter, bond length, granular distance) and $l$ is an external characteristic length (such as crack length, wave length); in addition, $e_0$ is a material-dependent constant [48]. Nonlocal effect considered in the nonlocal elasticity theory is determined by the magnitude of nonlocal parameter $\mu = e_0 a$ .

Using Hamilton's principle, nonlocal governing equations can be derived for the free vibration behavior of CCNTs.

$$\int_{t_0}^{t} \delta L \; \mathrm{d}t = 0 \qquad ; \qquad L = U_s - T^{NL} \tag{10}$$

where $U_s$ and $T^{NL}$ are strain energy and nonlocal kinematic energy. The $U_s$ is expressed as follows:

$$U_s = \frac{1}{2}\int_\Omega \sigma^{ij}\,\delta e_{ij}\,\mathrm{d}\Omega = \frac{1}{2}\int_\Omega \left[\sigma_s\, e_{ss} + 2\tau_{s\xi}\, e_{s\xi} + 2\tau_{s\eta}\, e_{s\eta}\right]\mathrm{d}\Omega \tag{11}$$

In this research, unlike the conventional method to convert local to nonlocal relations, the method introduced by Challamel et al. [49] and Hache [50] is adopted. That way, $T^{NL}$ is defined as follows:

$$T^{NL} = T + T^{Er} \tag{12}$$

where $T$ is kinematic energy and $T^{Er}$ is Eringen kinematic energy, which are expressed as follows:

$$T = \frac{1}{2}\int_\Omega \rho\left[\dot{W}^2 + \dot{U}^2 + \dot{V}^2\right]\mathrm{d}\Omega \tag{13}$$

$$T^{Er} = \frac{\mu^2}{2}\int_\Omega \rho\left[\left(\frac{\partial \dot{W}}{\partial s}\right)^2 + \left(\frac{\partial \dot{U}}{\partial s}\right)^2 + \left(\frac{\partial \dot{V}}{\partial s}\right)^2\right]\mathrm{d}\Omega \tag{14}$$

It is worth noting that Eringen kinematic energy $T^{Er}$ has no physical meaning [50]. The variations of $U_s$, $T$ and $T^{Er}$ are:

$$\begin{aligned}
\delta U_s &= \int_s\int_\xi\int_\eta \left[\sigma_s\,\delta e_{ss} + \tau_{s\xi}\,\delta(2e_{s\xi}) + \tau_{s\eta}\,\delta(2e_{s\eta})\right]\sqrt{g}\,\mathrm{d}s\,\mathrm{d}\xi\,\mathrm{d}\eta \\
\delta T &= \int_s\int_\xi\int_\eta \rho\left[\dot{W}\,\delta\dot{W} + \dot{U}\,\delta\dot{U} + \dot{V}\,\delta\dot{V}\right]\sqrt{g}\,\mathrm{d}s\,\mathrm{d}\xi\,\mathrm{d}\eta \\
\delta T^{Er} &= \mu^2\int_s\int_\xi\int_\eta \rho\left[\left(\frac{\partial \dot{W}}{\partial s}\right)\delta\left(\frac{\partial \dot{W}}{\partial s}\right) + \left(\frac{\partial \dot{U}}{\partial s}\right)\delta\left(\frac{\partial \dot{U}}{\partial s}\right) + \left(\frac{\partial \dot{V}}{\partial s}\right)\delta\left(\frac{\partial \dot{V}}{\partial s}\right)\right]\sqrt{g}\,\mathrm{d}s\,\mathrm{d}\xi\,\mathrm{d}\eta
\end{aligned} \tag{15}$$

where $g = (1 - \xi k_\eta + \eta k_\xi)^2$ is determinant of the metric tensor in the curvilinear coordinate system. To guarantee the first assumption $\sqrt{g} \approx 1$ [44, 45]. By substituting Eq. (15) into (10) and applying the Eqs. (2)-(4), the equilibrium equations are obtained by integrating as follows:

$$\begin{aligned}
\delta u_s &: \quad Q_s' - k_\eta Q_\xi + k_\xi Q_\eta = \left(1 - \mu^2\frac{\partial^2}{\partial s^2}\right)\rho A\,\ddot{u}_s \\
\delta u_\xi &: \quad Q_\xi' - k_s Q_\eta + k_\eta Q_s = \left(1 - \mu^2\frac{\partial^2}{\partial s^2}\right)\rho A\,\ddot{u}_\xi \\
\delta u_\eta &: \quad Q_\eta' - k_\xi Q_s + k_s Q_\xi = \left(1 - \mu^2\frac{\partial^2}{\partial s^2}\right)\rho A\,\ddot{u}_\eta \\
\delta \phi_s &: \quad M_s' - k_\eta M_\xi + k_\xi M_\eta = \left(1 - \mu^2\frac{\partial^2}{\partial s^2}\right)\rho I_p\,\ddot{\phi}_s \\
\delta \phi_\xi &: \quad M_\xi' - k_s M_\eta + k_\eta M_s - Q_\eta = \left(1 - \mu^2\frac{\partial^2}{\partial s^2}\right)\rho I_\xi\,\ddot{\phi}_\xi \\
\delta \phi_\eta &: \quad M_\eta' - k_\xi M_s + k_s M_\xi + Q_\xi = \left(1 - \mu^2\frac{\partial^2}{\partial s^2}\right)\rho I_\eta\,\ddot{\phi}_\eta
\end{aligned} \tag{16}$$

The associated boundary conditions are:

$$\begin{aligned}
&\left[Q_s+\mu^2\rho A\left(\frac{\partial \ddot{u}_s}{\partial s}\right)\right]\delta u_s\Big|_0^s=0\\
&\left[Q_\xi+\mu^2\rho A\left(\frac{\partial \ddot{u}_\xi}{\partial s}\right)\right]\delta u_\xi\Big|_0^s=0\\
&\left[Q_\eta+\mu^2\rho A\left(\frac{\partial \ddot{u}_\eta}{\partial s}\right)\right]\delta u_\eta\Big|_0^s=0\\
&\left[M_s+\mu^2\rho I_p\left(\frac{\partial \ddot{\phi}_s}{\partial s}\right)\right]\delta \phi_s\Big|_0^s=0\\
&\left[M_\xi+\mu^2\rho I_\xi\left(\frac{\partial \ddot{\phi}_\xi}{\partial s}\right)\right]\delta \phi_\xi\Big|_0^s=0\\
&\left[M_\eta+\mu^2\rho I_\eta\left(\frac{\partial \ddot{\phi}_\eta}{\partial s}\right)\right]\delta \phi_\eta\Big|_0^s=0
\end{aligned} \tag{17}$$

where two dots over the quantities denote the second partial derivative with respect to time *t*. $Q_s, Q_\xi$ and $Q_\eta$ are the axial and shear resultant forces and $M_s, M_\xi$ and $M_\eta$ are the twisting and bending resultant moments on a cross-section of the CCNTs which are defined as:

$$\begin{Bmatrix}Q_s\\Q_\xi\\Q_\eta\end{Bmatrix}=\iint_{\xi\,\eta}\begin{Bmatrix}\sigma_s\\\tau_{s\xi}\\\tau_{s\eta}\end{Bmatrix}d\xi\,d\eta \quad ; \quad \begin{Bmatrix}M_s\\M_\xi\\M_\eta\end{Bmatrix}=\iint_{\xi\,\eta}\begin{Bmatrix}\tau_{s\eta}\,\xi-\tau_{s\xi}\,\eta\\\sigma_s\,\eta\\-\sigma_s\,\xi\end{Bmatrix}d\xi\,d\eta \tag{18}$$

where $\rho, A, I_\xi, I_\eta$ and $I_p$ are the density, the cross-sectional area, the second moments of area and the torsional moment of inertia of the cross-section, respectively.

$$A=\iint_{\xi\,\eta}d\xi\,d\eta \quad ; \quad I_\xi=\iint_{\xi\,\eta}\eta^2\,d\xi\,d\eta \quad ; \quad I_\eta=\iint_{\xi\,\eta}\xi^2\,d\xi\,d\eta \quad ; \quad I_p=I_\xi+I_\eta \tag{19}$$

Finally, by substituting Eq. (18) in terms of displacement components into the equilibrium equations given in Eq. (16), the governing equations of motion for the CCNTs are obtained as follows:

$$\begin{aligned}
&EA(u_s''-k_\eta u_\xi')-k_\eta\left[G_\xi GA(u_\xi'+k_\eta u_s-k_s u_\eta-\phi_\eta)\right]=\left(1-\mu^2\frac{\partial^2}{\partial s^2}\right)\rho A\,\ddot{u}_s\\
&G_\xi GA(u_\xi''+k_\eta u_s'-k_s u_\eta'-\phi_\eta')-k_s\left[G_\eta GA(u_\eta'+k_s u_\xi+\phi_\xi)\right]+k_\eta\left[EA(u_s'-k_\eta u_\xi)\right]=\left(1-\mu^2\frac{\partial^2}{\partial s^2}\right)\rho A\,\ddot{u}_\xi\\
&G_\eta GA(u_\eta''+k_s u_\xi'+\phi_\xi')+k_s\left[G_\xi GA(u_\xi'+k_\eta u_s-k_s u_\eta-\phi_\eta)\right]=\left(1-\mu^2\frac{\partial^2}{\partial s^2}\right)\rho A\,\ddot{u}_\eta
\end{aligned} \tag{20}$$

$$GI_p(\phi_s'' - k_\eta \phi_\xi') - k_\eta\left[EI_\xi(\phi_\xi' + k_\eta \phi_s - k_s \phi_\eta)\right] = \left(1-\mu^2\frac{\partial^2}{\partial s^2}\right)\rho I_p \ddot{\phi}_s$$

$$EI_\xi(\phi_\xi'' + k_\eta \phi_s' - k_s \phi_\eta') - k_s\left[EI_\eta(\phi_\eta' + k_s \phi_\xi)\right] + k_\eta\left[GI_p(\phi_s' - k_\eta \phi_\xi)\right] -$$

$$-\left[G_\eta GA\ (u_\eta' + k_s u_\xi + \phi_\xi)\right] = \left(1-\mu^2\frac{\partial^2}{\partial s^2}\right)\rho I_\xi \ddot{\phi}_\xi$$

$$EI_\eta(\phi_\eta'' + k_s \phi_\xi') + k_s\left[EI_\xi(\phi_\xi' + k_\eta \phi_s - k_s \phi_\eta)\right] + \left[G_\xi GA(u_\xi' + k_\eta u_s - k_s u_\eta - \phi_\eta)\right] = \left(1-\mu^2\frac{\partial^2}{\partial s^2}\right)\rho I_\eta \ddot{\phi}_\eta$$

The clamped-clamped boundary conditions for CCNTs at $s = 0, l$ are as follows:

$$u_s = 0,\quad u_\xi = 0,\quad u_\eta = 0,\quad \phi_s = 0,\quad \phi_\xi = 0,\quad \phi_\eta = 0. \tag{21}$$

For an infinitesimal angular element, $\mathrm{d}s = C\,\mathrm{d}\beta$, the differential operator D is defined as follows in order to obtain the dimensionless form of governing equations of motion [44]:

$$\mathrm{D} = C\frac{\partial}{\partial s} = \frac{\partial}{\partial \beta} \quad ; \quad \mathrm{D}^2 = C^2\frac{\partial^2}{\partial s^2} = \frac{\partial^2}{\partial \beta^2} \tag{22}$$

Also, assuming the occurrence of harmonic vibration with the frequency of $\omega$, translational and rotational displacements can be expressed as follows:

$$u_\gamma(s,t) = \bar{u}_\gamma(s)e^{i\omega t} \quad ; \quad \phi_\gamma(s,t) = \bar{\phi}_\gamma(s)e^{i\omega t} \quad ; \quad \gamma = s, \xi, \eta \tag{23}$$

Using the Eqs. (22) and (23), the nonlocal governing equations of motion in the dimensionless form is obtained as follows:

$$\begin{aligned}
&(\mathrm{D}^2 - \lambda_{A1})\bar{u}_s(\beta) - \lambda_{A2}\,\mathrm{D}\bar{u}_\xi(\beta) + \lambda_{A3}\bar{u}_\eta(\beta) + C\,\lambda_{A4}\bar{\phi}_\eta(\beta) = -\lambda_{A5}\left(1-\frac{\mu^2}{C^2}\mathrm{D}^2\right)\bar{u}_s(\beta)\\
&(\mathrm{D}^2 - \lambda_{B1})\bar{u}_\xi(\beta) + \lambda_{B2}\,\mathrm{D}\bar{u}_s(\beta) - (\lambda_{B3} + \lambda_{B4})\mathrm{D}\bar{u}_\eta(\beta) - C\,\lambda_{B5}\bar{\phi}_\xi(\beta) - C\,\mathrm{D}\bar{\phi}_\eta(\beta) = -\lambda_{B6}\left(1-\frac{\mu^2}{C^2}\mathrm{D}^2\right)\bar{u}_\xi(\beta)\\
&(\mathrm{D}^2 - \lambda_{C1})\bar{u}_\eta(\beta) + \lambda_{C2}\bar{u}_s(\beta) + (\lambda_{C3} + \lambda_{C4})\mathrm{D}\bar{u}_\xi(\beta) + C\,\mathrm{D}\bar{\phi}_\xi(\beta) - C\,\lambda_{C5}\bar{\phi}_\eta(\beta) = -\lambda_{C6}\left(1-\frac{\mu^2}{C^2}\mathrm{D}^2\right)\bar{u}_\eta(\beta)\\
&(\mathrm{D}^2 - \lambda_{D1})\bar{\phi}_s(\beta) - \lambda_{D2}\,\mathrm{D}\bar{\phi}_\xi(\beta) + \lambda_{D3}\bar{\phi}_\eta(\beta) = -\lambda_{D4}\left(1-\frac{\mu^2}{C^2}\mathrm{D}^2\right)\bar{\phi}_s(\beta)\\
&C(\mathrm{D}^2 - \lambda_{E1})\bar{\phi}_\xi(\beta) + C\,\lambda_{E2}\,\mathrm{D}\bar{\phi}_s(\beta) - C\,\lambda_{E3}\,\mathrm{D}\bar{\phi}_\eta(\beta) - \lambda_{E4}\bar{u}_\xi(\beta) - \lambda_{E5}\,\mathrm{D}\bar{u}_\eta(\beta) = -C\,\lambda_{E6}\left(1-\frac{\mu^2}{C^2}\mathrm{D}^2\right)\bar{\phi}_\xi(\beta)\\
&C(\mathrm{D}^2 - \lambda_{F1})\bar{\phi}_\eta(\beta) + C\,\lambda_{F2}\bar{\phi}_s(\beta) + C\,\lambda_{F3}\,\mathrm{D}\bar{\phi}_\xi(\beta) + \lambda_{F4}\bar{u}_s(\beta) + \lambda_{F5}\,\mathrm{D}\bar{u}_\xi(\beta) - \lambda_{F6}\bar{u}_\eta(\beta) = -C\,\lambda_{F7}\left(1-\frac{\mu^2}{C^2}\mathrm{D}^2\right)\bar{\phi}_\eta(\beta)
\end{aligned} \tag{24}$$

In Eq. (24), the dimensionless quantities $\lambda_{A1}, \lambda_{A2}, ..., \lambda_{F7}$ are defined as:

$$\begin{aligned}
&\lambda_{A1} = \frac{C^2 k_\eta^2 G_\xi G}{E} \ ; \ \lambda_{A2} = \frac{C k_\eta (G_\xi G + E)}{E} \ ; \ \lambda_{A3} = \frac{C^2 k_\eta k_s G_\xi G}{E} \ ; \ \lambda_{A4} = \frac{C\,k_\eta G_\xi G}{E}\\
&\lambda_{A5} = \frac{C^2 \rho \omega^2}{E} \ ; \ \lambda_{B1} = \frac{C^2(k_s^2 G_\eta G + k_\eta^2 E)}{G_\xi G} \ ; \ \lambda_{B2} = \frac{C\,k_\eta (G_\xi G + E)}{G_\xi G} \ ; \ \lambda_{B3} = C\,k_s
\end{aligned} \tag{25}$$

$$\lambda_{B4}=\frac{C\,k_s G_\eta G}{G_\xi G}\;;\lambda_{B5}=\frac{C\,k_s G_\eta G}{G_\xi G};\lambda_{B6}=\frac{C^2\rho\omega^2}{G_\xi G}\;;\lambda_{C1}=\frac{C^2 k_s^2 G_\xi G}{G_\eta G}\;;\lambda_{C2}=\frac{C^2 k_\eta k_s G_\xi G}{G_\eta G}$$

$$\lambda_{C3}=C\,k_s\;\;;\;\;\lambda_{C4}=\frac{C\,k_s G_\xi G}{G_\eta G}\;\;;\;\;\lambda_{C5}=\frac{C\,k_s G_\xi G}{G_\eta G}\;\;;\;\;\lambda_{C6}=\frac{C^2\rho\omega^2}{G_\eta G}\;\;;\;\;\lambda_{D1}=\frac{C^2 k_\eta^2 EI_\xi}{GI_p}$$

$$\lambda_{E1}=\frac{C^2\left[k_s^2 EI_\eta+k_\eta^2 GI_P+G_\eta GA\right]}{EI_\xi}\;\;;\;\;\lambda_{E2}=\frac{C\,k_\eta(GI_p+EI_\xi)}{EI_\xi}\;\;;\;\;\lambda_{E3}=\frac{C\,k_s EI_p}{EI_\xi}$$

$$\lambda_{E4}=\frac{C^3 k_s G_\eta GA}{EI_\xi}\;;\;\;\lambda_{E5}=\frac{C^2 G_\eta GA}{EI_\xi}\;;\;\;\lambda_{E6}=\frac{C^2\rho\omega^2}{E}\;;\;\;\lambda_{F1}=\frac{C^2\left[k_s^2 EI_\xi+G_\xi GA\right]}{EI_\eta}$$

$$\lambda_{E4}=\frac{C^3 k_s G_\eta GA}{EI_\xi}\;;\;\;\lambda_{E5}=\frac{C^2 G_\eta GA}{EI_\xi}\;;\;\;\lambda_{E6}=\frac{C^2\rho\omega^2}{E}\;;\;\;\lambda_{F1}=\frac{C^2\left[k_s^2 EI_\xi+G_\xi GA\right]}{EI_\eta}$$

$$\lambda_{F6}=\frac{C^3 k_s G_\xi GA}{EI_\eta}\;\;;\;\;\lambda_{F7}=\frac{C^2\rho\omega^2}{E}$$

## 3 SOLUTION PROCEDURE

In this section, numerical solution is introduced to solve nonlocal governing equations for free vibrational responses of CCNTs. For this purpose, the generalized differential quadrature method (GDQM), which is an efficient and accurate numerical tool is used. The basic idea of GDQM is that the derivative of a function with respect to a coordinate variable at a given grid point can be approximated as the linear weighted sums of its values at all of the grid points in the domain. Based on GDQM, a typical function $f(\beta)$ with the domain of $0\le\beta\le\beta_0$ is discretized into $N$ grid points along the $\beta$-direction. Then, at each grid point of $\beta_i$, where $i=1,2,3,\ldots,N$, the *rth*-order partial derivatives of the $f(\beta)$ function with respect to $\beta$ are approximated as [51, 52]:

$$\left.\frac{\partial^r f(\beta)}{\partial\beta^r}\right|_{\beta=\beta_i}=\sum_{j=1}^{N}A_{ij}^{(r)}f_j \tag{26}$$

where $f_j=f(\beta_j)$, also the elements of $A_{ij}^{(r)}$ are the GDQ weighting coefficients of *rth*-order derivatives, which can be found in Ref. [51]. Unequally spaced grid points gives more accurate results, therefore, Gauss-Lobatto-Chebyshev type points is an appropriate choice [51], which is given as:

$$\beta_i=\frac{1}{2}\beta_0\left[1-\cos\frac{(i-1)\pi}{N-1}\right]\qquad,\qquad\beta_0=2n_p\pi \tag{27}$$

where $n_p$ is the number of pitches. Generally, dimensionless nonlocal governing equations by Eq. (24) are of Twelfth-order (6 coupled second-order equations) along with 12 boundary conditions at boundary points as given by Eq. (21). The GDQ approximation of Eq. (24) is written as:

$$\sum_{j=1}^{N}A_{ij}^{(2)}\bar{u}_{sj}-\lambda_{A1}\bar{u}_{si}-\lambda_{A2}\sum_{j=1}^{N}A_{ij}^{(1)}\bar{u}_{\xi j}+\lambda_{A3}\bar{u}_{\eta i}+C\,\lambda_{A4}\bar{\phi}_{\eta i}=-\lambda_{A5}\left(\bar{u}_{si}-\frac{\mu^2}{C^2}\sum_{j=1}^{N}A_{ij}^{(2)}\bar{u}_{sj}\right) \tag{28}$$

$$\sum_{j=1}^{N} A_{ij}^{(2)} \bar{u}_{\xi j} - \lambda_{B1} \bar{u}_{\xi i} + \lambda_{B2} \sum_{j=1}^{N} A_{ij}^{(1)} \bar{u}_{sj} - (\lambda_{B3} + \lambda_{B4}) \sum_{j=1}^{N} A_{ij}^{(1)} \bar{u}_{\eta j} - C\, \lambda_{B5} \bar{\phi}_{\xi i} - C \sum_{j=1}^{N} A_{ij}^{(1)} \bar{\phi}_{\eta j}$$
$$= -\lambda_{B6} \left( \bar{u}_{\xi i} - \frac{\mu^2}{C^2} \sum_{j=1}^{N} A_{ij}^{(2)} \bar{u}_{\xi j} \right)$$

$$\sum_{j=1}^{N} A_{ij}^{(2)} \bar{u}_{\eta j} - \lambda_{C1} \bar{u}_{\eta i} + \lambda_{C2} \bar{u}_{si} + \left( \lambda_{C3} + \lambda_{C4} \right) \sum_{j=1}^{N} A_{ij}^{(1)} \bar{u}_{\xi j} + C \sum_{j=1}^{N} A_{ij}^{(1)} \bar{\phi}_{\xi j} - C\, \lambda_{C5} \bar{\phi}_{\eta j}$$
$$= -\lambda_{C6} \left( \bar{u}_{\eta i} - \frac{\mu^2}{C^2} \sum_{j=1}^{N} A_{ij}^{(2)} \bar{u}_{\eta j} \right)$$

$$\sum_{j=1}^{N} A_{ij}^{(2)} \bar{\phi}_{sj} - \lambda_{D1} \bar{\phi}_{si} - \lambda_{D2} \sum_{j=1}^{N} A_{ij}^{(1)} \bar{\phi}_{\xi j} + \lambda_{D3} \bar{\phi}_{\eta i} = -\lambda_{D4} \left( \bar{\phi}_{si} - \frac{\mu^2}{C^2} \sum_{j=1}^{N} A_{ij}^{(2)} \bar{\phi}_{sj} \right)$$

$$C \sum_{j=1}^{N} A_{ij}^{(2)} \bar{\phi}_{\xi j} - \lambda_{E1} \bar{\phi}_{\xi i} + C\, \lambda_{E2} \sum_{j=1}^{N} A_{ij}^{(1)} \bar{\phi}_{sj} - C\, \lambda_{E3} \sum_{j=1}^{N} A_{ij}^{(1)} \bar{\phi}_{\eta j} - \lambda_{E4} \bar{u}_{\xi i} - \lambda_{E5} \sum_{j=1}^{N} A_{ij}^{(1)} \bar{u}_{\eta j}$$
$$= -C\, \lambda_{E6} \left( \bar{\phi}_{\xi i} - \frac{\mu^2}{C^2} \sum_{j=1}^{N} A_{ij}^{(2)} \bar{\phi}_{\xi j} \right)$$

$$C \sum_{j=1}^{N} A_{ij}^{(2)} \bar{\phi}_{\eta j} - \lambda_{F1} \bar{\phi}_{\eta i} + C\, \lambda_{F2} \bar{\phi}_{sj} + C\, \lambda_{F3} \sum_{j=1}^{N} A_{ij}^{(1)} \bar{\phi}_{\xi j} + \lambda_{F4} \bar{u}_{si} + \lambda_{F5} \sum_{j=1}^{N} A_{ij}^{(1)} \bar{u}_{\xi j} - \lambda_{F5} \bar{u}_{\eta i}$$
$$= -C\, \lambda_{F6} \left( \bar{\phi}_{\eta i} - \frac{\mu^2}{C^2} \sum_{j=1}^{N} A_{ij}^{(2)} \bar{\phi}_{\eta j} \right)$$

In addition, the GDQ approximation of boundary conditions from Eq. (21) at the $\beta = 0$ and $\beta = 2 n_p \pi$, boundary points are written as:

$$\bar{u}_{si} = 0, \quad \bar{u}_{\xi i} = 0, \quad \bar{u}_{\eta i} = 0, \quad \bar{\phi}_{si} = 0, \quad \bar{\phi}_{\xi i} = 0, \quad \bar{\phi}_{\eta i} = 0, \quad i = 1, N \tag{29}$$

In Eqs. (28) and (29), $\bar{u}_{\gamma i} = \bar{u}_{\gamma}(\beta_i)$, $\bar{\phi}_{\gamma i} = \bar{\phi}_{\gamma}(\beta_i)$, $\gamma = s, \xi, \eta$. The GDQ approximation of Eqs. (28) and (29) can be written in the matrix form as follows:

$$\begin{bmatrix} [K_{dd}] & [K_{db}] \\ [K_{bd}] & [K_{bb}] \end{bmatrix}_{6N \times 6N} \begin{Bmatrix} \{\delta_d\} \\ \{\delta_b\} \end{Bmatrix}_{6N \times 1} = \omega^2 \begin{Bmatrix} [M_d]\{\delta_d\} \\ \{\delta_d\} \end{Bmatrix}_{6N \times 1} \tag{30}$$

where the subscripts *b* and *d* refer to the boundary and domain grid points, respectively. The elements of the stiffness matrixes $[K_{dd}]$ and $[K_{db}]$ and the mass matrix $[M_d]$ are obtained from the GDQ approximations of the governing equations of motion; while the elements of the stiffness matrixes $[K_{bd}]$ and $[K_{bb}]$ are obtained from the GDQ approximations of boundary conditions. The displacement vectors of $\{\delta_d\}$ and $\{\delta_b\}$ are defined by:

$$\{\delta_d\} = \{ \bar{u}_{sd} \;\; \bar{u}_{\xi d} \;\; \bar{u}_{\eta d} \;\; \bar{\phi}_{sd} \;\; \bar{\phi}_{\xi d} \;\; \bar{\phi}_{\eta d} \}^T$$
$$\{\delta_b\} = \{ \bar{u}_{sb} \;\; \bar{u}_{\xi b} \;\; \bar{u}_{\eta b} \;\; \bar{\phi}_{sb} \;\; \bar{\phi}_{\xi b} \;\; \bar{\phi}_{\eta b} \}^T \tag{31}$$

Finally, by solving the eigenvalue system of Eq. (30), the natural frequencies of $\omega$ and the associated mode shapes of the CCNTs will be obtained.

## 4 RESULTS AND DISCUSSION

Since the free vibration of helical nano-beams and CCNTs has not been studied from the continuum mechanics point of view; therefore for validating the proposed method, a helical spring sample that its vibrational behavior has already been studied under clamped-clamped boundary conditions in the experimental [37] and theoretical [39, 44] investigations, is considered. The geometric and material characteristics of this helical spring sample are as follows:

$$\rho = 7900 kg/m^3, \quad E = 2.06\times10^{11} N/m^2, \quad \nu = 0.3, \quad D = 2R = 10 mm, \quad d = 1 mm, \quad n_p = 7.6, \\ \bar{\alpha} = 8.5744°, \quad G_\xi = G_\eta = 0.9091 \tag{32}$$

where *D, d* and *v* the centerline diameter of the helix, the diameter of cross-section and Poisson's ratio, respectively. By setting nonlocal parameter $\mu = 0$, the present method is reduced to the local continuum model of the mentioned helical spring sample. As provided in Table 1, the present results are in very good agreement with the results given by Mottershead [37], Yildirim [39] and Yu et al. [44].

**Table 1**
Comparison of natural frequencies (*Hz*) of the helical spring with circular cross-section under clamped-clamped BCs.

| Modes | $f_1$ | $f_2$ | $f_3$ | $f_4$ | $f_5$ | $f_6$ | $f_7$ | $f_8$ | $f_9$ |
|---|---|---|---|---|---|---|---|---|---|
| Mottershead [37] | 391.0 | 391.0 | 459.0 | 528.0 | 878.0 | 878.0 | 906.0 | ---- | 1282.0 |
| Yildirim [39] | 393.5 | 395.9 | 462.8 | 525.5 | 864.0 | 876.8 | 914.3 | 1037.0 | 1310.5 |
| Yu et al. [44] | 393.5 | 396.1 | 462.9 | 525.7 | 863.8 | 877.0 | 913.8 | 1037.5 | 1310.7 |
| Present study | 393.4 | 396.0 | 462.7 | 525.6 | 863.6 | 876.8 | 913.5 | 1037.2 | 1310.4 |

In this study, according to Fig.3, various CCNT samples are built from armchair single-walled CNTs (5,5). To guarantee the first assumption $D/d \geq 4$, $k_\eta \leq 0.4888\ nm^{-1}$ are for the CCNTs.

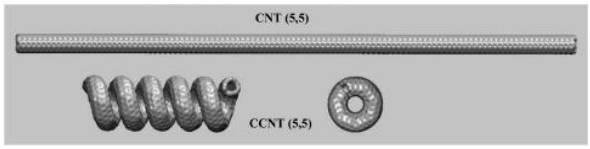


**Fig.3**
Single-walled carbon nanotube CNT (5,5) and coiled carbon nanotube CCNT (5,5).

Zhang et al. [53] reported the geometric and material characteristics of the CNT (5,5) as follow:

$$E/\rho = 3.6481\times10^8\ m^2/s^2, \quad E\,t = 278.25 GPa\,nm, \quad \nu = 0.19, \quad d = 0.678 nm \tag{33}$$

Using MD simulation for the free longitudinal vibration of the CNT (5,5), they concluded that the $E/\rho$ ratio is constant and independent of CNTs length [53]. *t* is wall thickness of the CNTs. Conventionally, the interlayer spacing of graphite i.e., $t = 0.34\ nm$, is taken as the CNTs thickness [53]. The $\rho, E$ and $G$ values of CCNTs (5,5) are obtained as follows:

$$\rho = \frac{N_{\text{atom}}\, m}{A\, L}, \quad E = 3.6481\times10^8 \rho, \quad G = \frac{E}{2(1+\nu)} \tag{34}$$

where $N_{\text{atom}}$ is the number of atoms and *m* is mass of a carbon atom that is equal to $1.99452\times10^8\ gr$. Additionally, *L* is the total helix length of the desired CCNT (5,5) that is identical with the length of the CNT, which can be obtained through the following equation:

$$L = \pi D n_p \sqrt{1+\tan^2 \bar{\alpha}} \tag{35}$$

Using Eq. (19) the parameters $A, I_\xi, I_\eta$ for the CCNTs is obtained as follow:

$$A = \frac{\pi}{4}\left[(d+t)^2 - (d-t)^2\right] \quad ; \quad I_\xi = I_\eta = \frac{\pi}{64}\left[(d+t)^4 - (d-t)^4\right] \tag{36}$$

Furthermore, for the free vibration of CNT (5,5) under clamped-clamped boundary conditions, Arash and Ansari obtained the nonlocal parameter $\mu = 1.7\,nm$ based on nonlocal shell model [54] and using the results of the MD simulation [53]. In this study, the nonlocal parameter of the CCNTs with clamped-clamped boundary conditions is considered $\mu = 1.7\,nm$.

Values of helix length $L$ and number of atoms $N_{\text{atom}}$ of the CCNTs samples studied in this paper are provided in Tables 2-4.

**Table 2**
The helix length $L$ and number of atoms $N_{\text{atom}}$ of the CCNTs (5,5) with $E$=817.01 *GPa*, $v$=0.19, $G$=343.28 *GPa*, $\bar{\alpha} = 20.57°$, $n_p = 6$ and various ratio $D/d$.

| $D/d$ | 4 | 6 | 8 | 10 | 12 | 14 | 16 |
|---|---|---|---|---|---|---|---|
| $L(nm)$ | 54.601 | 81.902 | 109.202 | 136.503 | 163.803 | 191.104 | 218.405 |
| $N_{\text{atom}}$ | 4440 | 6660 | 8880 | 11100 | 13320 | 15540 | 17760 |

**Table 3**
The helix length $L$ and number of atoms $N_{\text{atom}}$ of the CCNTs (5,5) with $E$=817.01 *GPa*, $G$=343.28 *GPa*, $D/d = 4$, $\bar{\alpha} = 20.57°$ and various number of pitches $n_p$.

| $n_p$ | 2 | 4 | 6 | 8 | 10 | 12 | 14 | 16 | 18 |
|---|---|---|---|---|---|---|---|---|---|
| $L(nm)$ | 18.200 | 36.401 | 54.601 | 72.801 | 91.002 | 109.202 | 127.403 | 145.603 | 163.803 |
| $N_{\text{atom}}$ | 1480 | 2960 | 4440 | 5920 | 7400 | 8880 | 10360 | 11840 | 13320 |

**Table 4**
The helix length $L$ and number of atoms $N_{\text{atom}}$ of the CCNTs (5,5) with $E$=817.01 *GPa*, $v$=0.19, $G$=343.28 *GPa*, $D/d = 4$, $n_p = 6$ and various pitch angle $\bar{\alpha}$.

| $\bar{\alpha}$ | 11.36° | 15.79° | 20.57° | 25.35° | 30.00° | 34.43° | 38.61° |
|---|---|---|---|---|---|---|---|
| $L(nm)$ | 52.142 | 53.125 | 54.601 | 56.569 | 59.028 | 61.980 | 65.423 |
| $N_{\text{atom}}$ | 4240 | 4320 | 4440 | 4600 | 4800 | 5040 | 5320 |

For instance, the mode shapes for a CCNT (5,5) is plotted with $D/d = 4, n_p = 6, \bar{\alpha} = 20.57°$ and $\mu = 1.7\,nm$ under clamped-clamped boundary conditions (Fig. 4).

In Fig. 4, the first eight mode shapes of the CCNT (5,5) can be observed. Due to the stretching, bending and torsion deformations in the CCNTs, occurs longitudinal, transverse and torsional vibrational coupling. The fundamental mode shape of the CCNTs is always transvers. Mode 5 and 6 are predominantly longitudinal vibrational motions, while the other modes of the CCNT in Fig. 4 are predominantly transverse vibrational motions.

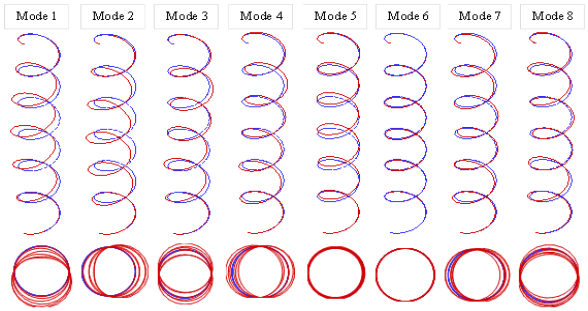


**Fig.4**
First eight mode shapes of the CCNT free vibration with $D/d=4, n_p=6, \bar{\alpha}=20.57°$ under clamped-clamped BCs. Solid line: deformed shape, Dotted line: undeformed shape.

Furthermore, coupled mode shapes with normalized translational displacements $(u_s, u_\xi, u_\eta)$ and rotations displacements $(\phi_s, \phi_\xi, \phi_\eta)$ of the CCNT shown in Figs. 5 and 6. It is worth noting, unlike the CNTs, increasing a pitch in the CCNTs appears a vibrating peak in the fundamental mode shape.

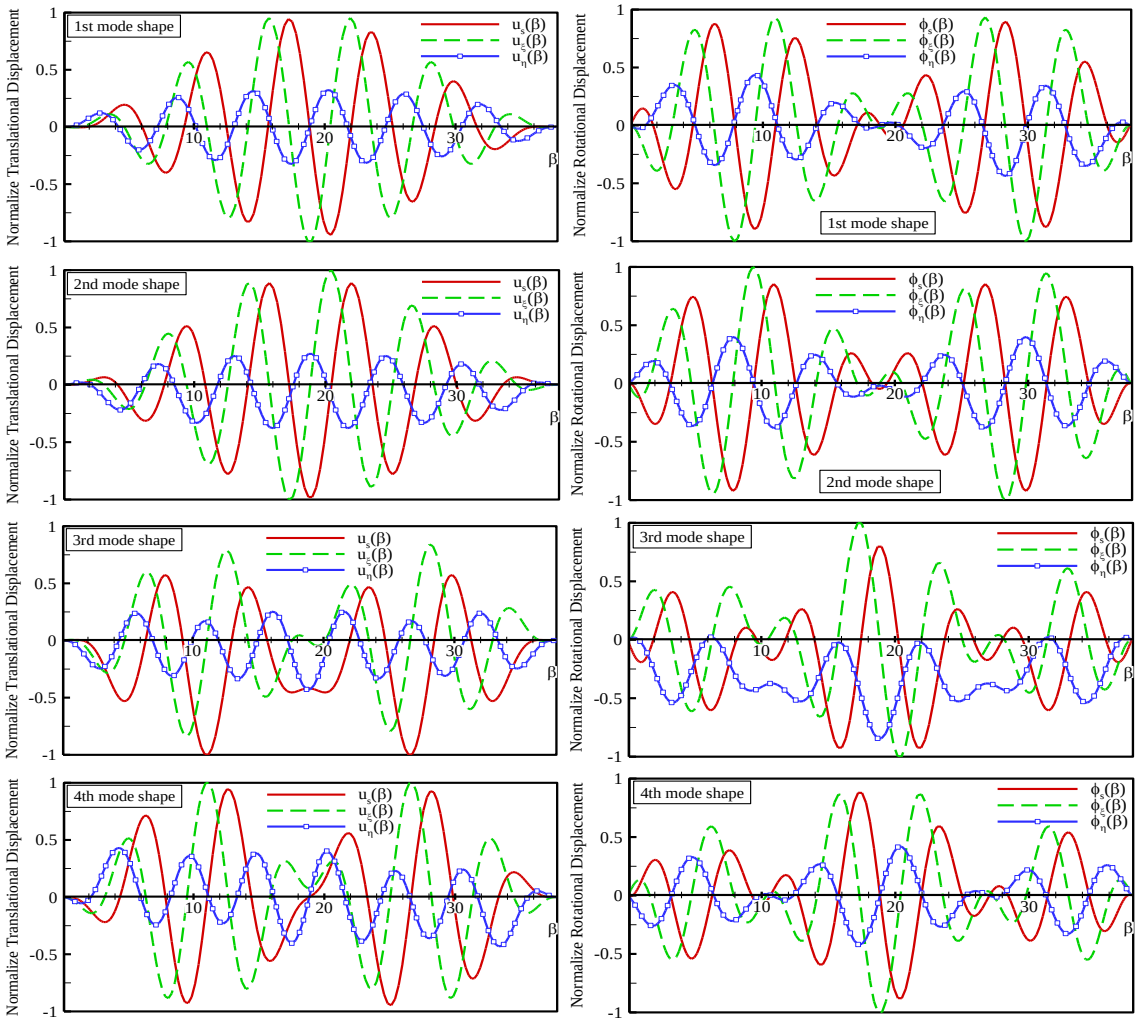


**Fig.5**
The first four mode shapes of the CCNT for normalized translations $(u_s, u_\xi, u_\eta)$ and rotations $(\phi_s, \phi_\xi, \phi_\eta)$ with $D/d=4$, $n_p=6, \bar{\alpha}=20.57°$ and $\mu=1.7\,nm$ under clamped-clamped BCs.

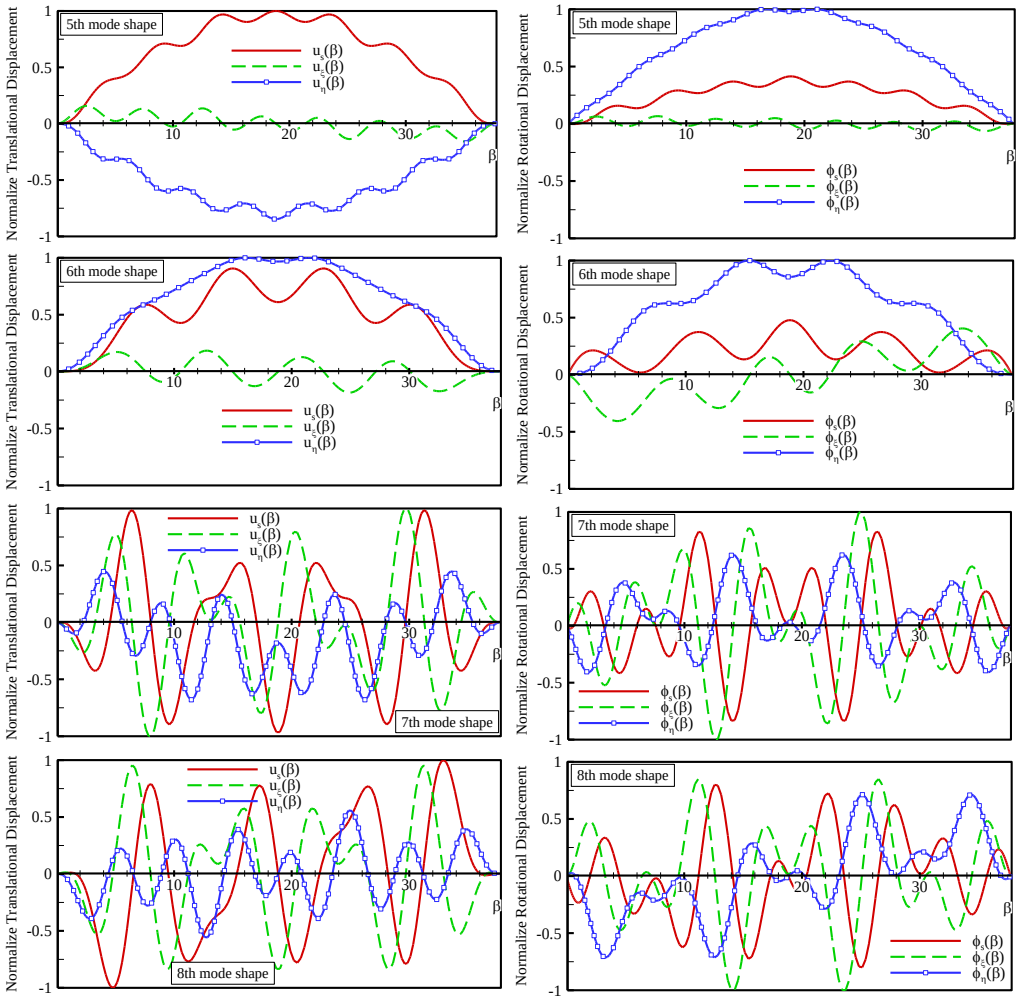


**Fig.6**
The second four mode shapes of the CCNT for normalized translations $(u_s, u_\xi, u_\eta)$ and rotations $(\phi_s, \phi_\xi, \phi_\eta)$ with $D/d = 4, n_p = 6, \bar{\alpha} = 20.57°$ and $\mu = 1.7\,nm$ under clamped-clamped BCs.

The natural frequencies of the CCNT (5,5) are given in Table 5. Regarding this Table, it is seen that some of the frequencies in CCNT are close to each other, which is in contrary with the elementary theory [35]. Therefore it can be concluded that a general instruction for determining the free vibration frequencies of CCNTs cannot be presented.

### *4.1 Effect of the nonlocal parameter*

Also, effect of the nonlocal parameter on the natural frequencies of CCNT (5,5) is reported in Table 5. As can observed, for the nonlocal parameter of $\mu = 1.7\,nm$, the natural frequencies of the CCNT decrease compared to $\mu = 0.0\,nm$ (i.e. local continuum model). This is because the nonlocal parameter decreases CCNTs stiffness and consequently the frequency values are reduced.

**Table 5**
The natural frequencies (*GHz*) of the CCNT (5,5) with $D/d = 4, n_p = 6, \bar{\alpha} = 20.57°$ under clamped-clamped BCs.

| $\mu = e_0 a$ | Modes | | | | | | | | |
|---|---|---|---|---|---|---|---|---|---|
| $(nm)$ | $f_1$ | $f_2$ | $f_3$ | $f_4$ | $f_5$ | $f_6$ | $f_7$ | $f_8$ | $f_9$ |
| 0.0 | 15.418 | 15.446 | 30.512 | 33.343 | 38.242 | 38.480 | 58.642 | 63.213 | 65.410 |
| 1.7 | 10.013 | 10.017 | 24.792 | 25.025 | 30.362 | 33.341 | 43.283 | 43.912 | 56.925 |

Furthermore, the nonlocal parameter can affect on the arrangement of CCNT mode shapes. To verify this claim, the mode shapes of the CCNT with $\mu = 0.0nm$ and $\mu = 1.7nm$ are plotted in Fig. 7.

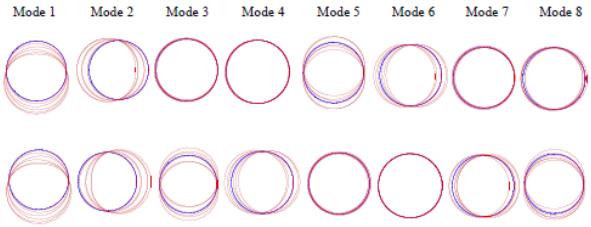


**Fig.7**
First eight mode shapes of the free vibration of the CCNT with $D/d = 4, n_p = 6, \bar{\alpha} = 20.57°$ under clamped-clamped BCs, (a) $\mu = 0.0nm$ and (b) $\mu = 1.7nm$.

The effect of the nonlocal parameter on the $f_1$ and $f_7$ natural frequencies of various CCNTs is shown in Figs. 8-10. As it is obvious, the nonlocal parameter reduces CCNTs natural frequency values. Moreover, by increasing the *D/d* ratio, number of pitches $n_p$ and helix pitch angle $\bar{\alpha}$, the effect of nonlocal parameter on the natural frequencies is decreased.

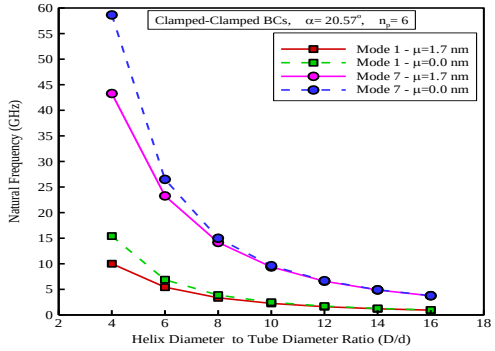


**Fig.8**
Effect of the nonlocal parameter on the natural frequencies (*GHz*) of the CCNTs with various *D/d* ratios.

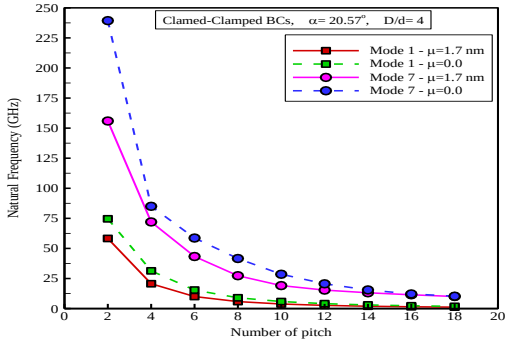


**Fig.9**
Effect of the nonlocal parameter on the natural frequencies (*GHz*) of the CCNTs with various number of pitches.

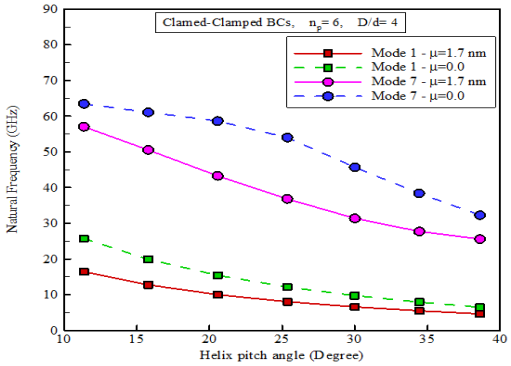


**Fig.10**
Effect of the nonlocal parameter on the natural frequencies (*GHz*) of the CCNTs with various helix pitch angles.

Here, the fundamental frequencies of the CNT (5,5) and the CCNT (5,5) are compared with same length and nonlocal parameter. The fundamental frequency of the CNT (5,5) was obtained $f_1 = 45.75\,\text{GHz}$ with $L = 19.184\,nm$ and $\mu = 1.7\,nm$ by Arash and Ansari [54], while the fundamental frequency of the CCNT (5,5) is $f_1 = 54.51\,\text{GHz}$ with same length ( $D/d = 4, \bar{\alpha} = 20.57°, n_p = 2.11$ ) and nonlocal parameter in the present study.

### *4.2 Effect of the ratio of D/d*

The variation of the natural frequencies versus the ratio of *D/d* is given in Table 6. As this ratio increases, decreasing trend can be observed in CCNTs stiffness, which in turn reduces the frequencies. Also, the frequencies get closer to each other with increasing this ratio and coupled modes begin to emerge.

**Table 6**
Effect of the ratio of *D/d* on the natural frequencies (*GHz*) of the CCNTs (5,5) with $n_p = 6, \bar{\alpha} = 20.57°, \mu = 1.7\,nm$ under clamped-clamped BCs.

| $D/d$ | Modes | | | | | | | | |
|---|---|---|---|---|---|---|---|---|---|
| | $f_1$ | $f_2$ | $f_3$ | $f_4$ | $f_5$ | $f_6$ | $f_7$ | $f_8$ | $f_9$ |
| 4 | 10.013 | 10.017 | 24.792 | 25.025 | 30.362 | 33.341 | 43.283 | 43.912 | 56.925 |
| 6 | 5.430 | 5.432 | 13.246 | 13.602 | 14.011 | 15.159 | 23.268 | 23.789 | 26.347 |
| 8 | 3.349 | 3.352 | 7.749 | 8.268 | 8.390 | 8.705 | 14.172 | 14.618 | 15.091 |
| 10 | 2.251 | 2.253 | 4.999 | 5.395 | 5.637 | 5.734 | 9.376 | 9.791 | 9.810 |
| 12 | 1.608 | 1.610 | 3.484 | 3.769 | 4.027 | 4.074 | 6.597 | 6.909 | 6.979 |
| 14 | 1.203 | 1.205 | 2.565 | 2.777 | 3.012 | 3.041 | 4.876 | 5.129 | 5.211 |
| 16 | 0.932 | 0.934 | 1.966 | 2.129 | 2.333 | 2.353 | 3.745 | 3.955 | 4.032 |

### *4.3 Effect of the number of pitches*

The variation of the natural frequencies versus the number of pitches $n_p$, is given Table 7. According to this table, increasing $n_p$ would lead to an increase in the helix length and decrease in the stiffness of the CCNTs. Consequently, the frequencies are reduced and coupled modes begin to appear.

**Table 7**
Effect of the number of pitches on the CCNTs (5,5) natural frequencies (*GHz*) with $D/d = 4, \bar{\alpha} = 20.57°, \mu = 1.7\,nm$ under clamped-clamped BCs.

| $n_p$ | Modes | | | | | | | | |
|---|---|---|---|---|---|---|---|---|---|
| | $f_1$ | $f_2$ | $f_3$ | $f_4$ | $f_5$ | $f_6$ | $f_7$ | $f_8$ | $f_9$ |
| 2 | 58.277 | 60.757 | 77.438 | 96.174 | 110.799 | 141.599 | 155.928 | 176.062 | 208.159 |
| 4 | 20.652 | 20.737 | 43.231 | 47.582 | 47.607 | 51.215 | 72.010 | 76.805 | 81.095 |
| 6 | 10.013 | 10.017 | 24.792 | 25.025 | 30.362 | 33.341 | 43.283 | 43.912 | 56.925 |
| 8 | 5.822 | 5.827 | 15.049 | 15.115 | 22.679 | 25.061 | 27.325 | 27.737 | 40.808 |
| 10 | 3.787 | 3.790 | 9.999 | 10.030 | 17.785 | 18.571 | 19.104 | 20.222 | 28.731 |
| 12 | 2.654 | 2.656 | 7.094 | 7.111 | 13.287 | 13.363 | 15.370 | 16.832 | 21.053 |
| 14 | 1.961 | 1.962 | 5.282 | 5.292 | 10.029 | 10.043 | 13.118 | 14.431 | 16.006 |
| 16 | 1.507 | 1.508 | 4.080 | 4.086 | 7.806 | 7.808 | 11.458 | 12.500 | 12.543 |
| 18 | 1.193 | 1.194 | 3.244 | 3.248 | 6.237 | 6.238 | 10.019 | 10.075 | 10.235 |

### *4.4 Effect of the helix pitch angle*

The variation of the frequencies with respect to the helix pitch angle $\bar{\alpha}$ is given in Table 8. As $\bar{\alpha}$ increases, the helix length increases and the stiffness of the CCNTs decreases, which reduces the frequencies, subsequently. Again, the occurrence of the coupled modes is begun with increasing $\bar{\alpha}$ .

**Table 8**
Effect of helix pitch angle on the CCNTs (5,5) natural frequencies (*GHz*) with $D/d=4,\quad n_p=6, \mu=1.7\,nm$ under clamped-clamped BCs.

| $\bar{\alpha}$ | Modes | | | | | | | | |
|---|---|---|---|---|---|---|---|---|---|
| | $f_1$ | $f_2$ | $f_3$ | $f_4$ | $f_5$ | $f_6$ | $f_7$ | $f_8$ | $f_9$ |
| 11.36° | 16.452 | 16.506 | 31.651 | 34.011 | 36.578 | 37.800 | 57.043 | 58.782 | 61.172 |
| 15.79° | 12.766 | 12.778 | 29.720 | 30.440 | 31.576 | 34.586 | 50.537 | 51.285 | 59.417 |
| 20.57° | 10.013 | 10.017 | 24.792 | 25.025 | 30.362 | 33.341 | 43.283 | 43.912 | 56.925 |
| 25.35° | 8.038 | 8.047 | 20.540 | 20.706 | 29.122 | 32.036 | 36.822 | 37.616 | 52.973 |
| 30.00° | 6.591 | 6.600 | 17.174 | 17.312 | 27.612 | 30.302 | 31.392 | 32.785 | 47.083 |
| 34.43° | 5.494 | 5.502 | 14.500 | 14.617 | 25.529 | 26.881 | 27.720 | 30.054 | 41.199 |
| 38.61° | 4.635 | 4.642 | 12.343 | 12.442 | 22.642 | 23.120 | 25.580 | 28.280 | 35.957 |

## 5 CONCLUSION

In this paper, for the first time a nonlocal continuum method were proposed to study free vibration behavior of the single-walled CCNTs. The free vibration equations were derived based on a nonlocal helical beam model, including Washizu's beam model and the nonlocal elasticity theory. Then, the nonlocal governing equations were solved numerically via GDQM. The vibrating natural frequencies and the corresponding mode shapes were obtained for CCNTs under clamped-clamped boundary conditions. Moreover, the effect of nonlocal parameter and the geometric parameters such as the ratio of *D/d*, the number of pitches and the helix pitches angle on the free vibrational behavior of the CCNTs were investigated and general conclusion were obtained. Thus, with increasing these parameters, the stiffness of the CCNTs was decreased and consequently, the natural frequencies were reduced as coupled modes begin to emerge. Also, it was found that the nonlocal parameter reduces the natural frequencies and changes the arrangement of the CCNTs mode shapes. Main limitation of present study is nonlocal parameter value of the CCNTs for different geometrical parameters such as diameter and chirality that must be determined by molecular dynamics simulation. Also, the curvature of CCNTs should be moderate. The present method can be used to investigate the effect of different boundary conditions, the tensile and compressive initial strain and axial static forces, attached mass and temperature on the free vibration behavior of CCNTs in future researches.

## REFERENCES

[1] Iijima S., 1991, Helical microtubules of graphitic carbon, *Nature* **354**: 56-58.
[2] Liu L., Liu F., Zhao J., 2014, Curved carbon nanotubes: From unique geometries to novel properties and peculiar applications, *Nano Research* **7**(5): 626-657.
[3] Ihara S., Itoh S., Kitakami J.-i., 1993, Helically coiled cage forms of graphitic carbon, *Physical Review B* **48**(8): 5643-5647.
[4] Biró L.P., Lazarescu S.D., Thiry P.A., Fonseca A., Nagy J.B., Lucas A.A., Lambin P., 2000, Scanning tunneling microscopy observation of tightly wound, single-wall coiled carbon nanotubes, *Europhysics Letters (EPL)* **50**(4): 494-500.
[5] Chang J.H., Park W., 2006, Nano elastic memory using carbon nanocoils, *Journal of Nanobiotechnology* **3**(1): 30-35.
[6] Volodin A., Buntinx D., Ahlskog M., Fonseca A., Nagy J.B., Van Haesendonck C., 2004, Coiled carbon nanotubes as self-sensing mechanical resonators, *Nano Letters* **4**(9): 1775-1779.
[7] Bell D.J., Sun Y., Zhang L., Dong L.X., Nelson B.J., Grutzmacher D., 2005, Three-dimensional nanosprings for electromechanical sensors, *The 13th International Conference on Solid-State Sensors, Actuators and Microsystems* **11**: 15-18.
[8] Hernadi K., Thiên-Nga L., Forró L., 2001, Growth and microstructure of catalytically produced coiled carbon nanotubes, *The Journal of Physical Chemistry B* **105**(50): 12464-12468.
[9] Lau K.T., Lu M., Hui D., 2006, Coiled carbon nanotubes: Synthesis and their potential applications in advanced composite structures, *Composites Part B: Engineering* **37**(6): 437-448.
[10] Wu J., He J., Odegard G.M., Nagao S., Zheng Q., Zhang Z., 2013, Giant stretchability and reversibility of tightly wound helical carbon nanotubes, *Journal of the American Chemical Society* **135**(37): 13775-13785.
[11] Behera L., Chakraverty S., 2017, Recent researches on nonlocal elasticity theory in the vibration of carbon nanotubes using beam models: A review, *Archives of Computational Methods in Engineering* **24**(3): 481-494.
[12] da Fonseca A.F., Galvão D.S., 2004, Mechanical properties of nanosprings, *Physical Review Letters* **92**(17): 175502.

[13] Liu L., Gao H., Zhao J., Lu J., 2010, Superelasticity of carbon nanocoils from atomistic quantum simulations, *Nanoscale Research Lett*ers **5**(3): 478-483.

[14] Ghaderi S.H., Hajiesmaili E., 2013, Nonlinear analysis of coiled carbon nanotubes using the molecular dynamics finite element method, *Materials Science and Engineering: A* **582**: 225-234.

[15] Wang J., Kemper T., Liang T., Sinnott S.B., 2012, Predicted mechanical properties of a coiled carbon nanotube, *Carbon* **50**(3): 968-976.

[16] Wu J., He J., Odegard G.M., Nagao S., Zheng Q., Zhang Z., 2013, Giant stretchability and reversibility of tightly wound helical carbon nanotubes, *Journal of the American Chemical Society* **135**(37): 13775-13785.

[17] Khani N., Yildiz M., Koc B., 2016, Elastic properties of coiled carbon nanotube reinforced nanocomposite: A finite element study, *Materials & Design* **109**: 123-132.

[18] Kianfar A., Seyyed Fakhrabadi M.M., Mashhadi M.M., 2019, Prediction of mechanical and thermal properties of polymer nanocomposites reinforced by coiled carbon nanotubes for possible application as impact absorbent, *Proceedings of the Institution of Mechanical Engineers, Part C: Journal of Mechanical Engineering Science* **234**(4): 882-902.

[19] Yarali E., Baniassadi M., Baghani M., 2019, Numerical homogenization of coiled carbon nanotube reinforced shape memory polymer nanocomposites, *Smart Materials and Structures* **28**(3): 035026.

[20] Fakhrabadi M.M.S., Amini A., Reshadi F., Khani N., Rastgoo A., 2013, Investigation of buckling and vibration properties of hetero-junctioned and coiled carbon nanotubes, *Computational Materials Science* **73**: 93-112.

[21] Rahmani O., Darvishi F., 2018, Investigation of the free longitudinal vibration of single-walled coiled carbon nanotubes (SWCCNTs) using molecular dynamics simulation, *Amirkabir Journal of Mechanical Engineering* **51**:1-3.

[22] Arash B., Wang Q., Wu N., 2012, Gene detection with carbon nanotubes, *Journal of Nanotechnology in Engineering and Medicine* **3**(2): 020902.

[23] Gajbhiye S.O., Singh S.P., 2015, Vibration characteristics of open- and capped-end single-walled carbon nanotubes using multi-scale analysis technique incorporating Tersoff–Brenner potential, *Acta Mechanica* **226**(11): 3565-3586.

[24] Ramezani Ali-Akbari H., Firouz-Abadi R., 2015, Nonlinear free vibration of single-walled carbon nanotubes embedded in viscoelastic medium based on asymptotic perturbation method, *Journal of Science and Engineering* **06**: 42-58.

[25] Farokhi H., Païdoussis M.P., Misra A.K., 2016, A new nonlinear model for analyzing the behaviour of carbon nanotube-based resonators, *Journal of Sound and Vibration* **378**: 56-75.

[26] Hussain M., Naeem M.N., 2017, Vibration analysis of single-walled carbon nanotubes using wave propagation approach, *International Journal of Mechanical Sciences* **8**(1): 155-164.

[27] Tadi Beni Y., Mehralian F., Karimi Zeverdejani M., 2017, Free vibration of anisotropic single-walled carbon nanotube based on couple stress theory for different chirality, *Journal of Low Frequency Noise, Vibration and Active Control* **36**(3): 277-293.

[28] Jiang J., Wang L., Zhang Y., 2017, Vibration of single-walled carbon nanotubes with elastic boundary conditions, *International Journal of Mechanical Sciences* **122**: 156-166.

[29] Shahabodini A., Ansari R., Darvizeh M., 2018, Atomistic-continuum modeling of vibrational behavior of carbon nanotubes using the variational differential quadrature method, *Composite Structures* **185**: 728-747.

[30] Chwał M., 2018, Nonlocal analysis of natural vibrations of carbon nanotubes, *Journal of Materials Engineering and Performance* **27**(11): 6087-6096.

[31] Eltaher M.A., Almalki T.A., Almitani K.H., Ahmed K.I.E., Abdraboh A.M., 2019, Modal participation of fixed–fixed single-walled carbon nanotube with vacancies, *International Journal of Advanced Structural Engineering* **11**(2): 151-163.

[32] Majeed A., Zeeshan A., Mubbashir S., 2019, Vibration analysis of carbon nanotubes based on cylindrical shell by inducting Winkler and Pasternak foundations, *Mechanics of Advanced Materials and Structures* **26**(13): 1140-1145.

[33] Hussain M., Naeem M.N., 2020, Mass density effect on vibration of zigzag and chiral SWCNTs: A theoretical study, *Journal of Sandwich Structures & Materials* DOI:10.1177/1099636220906257.

[34] Hayati H., Hosseini S.A., Rahmani O., 2017, Coupled twist–bending static and dynamic behavior of a curved single-walled carbon nanotube based on nonlocal theory, *Microsystem Technologies* **23**(7): 2393-2401.

[35] Wahl A.M., *1963, Mechanical Springs*, McGraw-Hill, New York.

[36] Wittrick W.H., 1966, On elastic wave propagation in helical springs, *International Journal of Mechanical Sciences* **8**(1): 25-47.

[37] Mottershead J.E., 1980, Finite elements for dynamical analysis of helical rods, *International Journal of Mechanical Sciences* **22**(5): 267-283.

[38] Pearson D., 1982, The transfer matrix method for the vibration of compressed helical springs, *Journal of Mechanical Engineering Science* **24**(4): 163-171.

[39] Yildirim V., 1996, Investigation of parameters affecting free vibration frequency of helical springs, *International Journal for Numerical Methods in Engineering* **39**(1): 99-114.

[40] Yildirim V., On the linearized disturbance dynamic equations for buckling and free vibration of cylindrical helical coil springs under combined compression and torsion, *Meccanica* **47**(4): 1015-1033.

[41] Yildirim V., 2016, Axial static load dependence free vibration analysis of helical springs based on the theory of spatially curved bars, *Latin American Journal of Solids and Structures* **13**: 2852-2875.

[42] Lee J., Thompson D.J., 2001, Dynamic stiffness formulation, free vibration and wave motion of helical springs, *Journal of Sound and Vibration* **239**(2): 297-320.
[43] Lee J., 2007, Free vibration analysis of cylindrical helical springs by the pseudospectral method, *Journal of Sound and Vibration* **302**(1): 185-196.
[44] Yu A.M., Yang C., 2010, Formulation and evaluation of an analytical study for cylindrical helical springs, *Acta Mechanica Solida Sinica* **23**(1): 85-94.
[45] Washizu K., 1964, Some considerations on a naturally curved and twisted slender beam, *Journal of Mathematics and Physics* **43**(1-4): 111-116.
[46] Timoshenko S.P., Goodier J.N., 1951, *Theory of Elasticity*, McGraw-HilI.
[47] Brancheriau L., 2006, Influence of cross section dimensions on Timoshenko's shear factor – Application to wooden beams in free-free flexural vibration, *Annals of Forest Science* **63**(3): 319-321.
[48] Eringen A.C., 1983, On differential equations of nonlocal elasticity and solutions of screw dislocation and surface waves, *Journal of Applied Physics* **54**(9): 4703-4710.
[49] Challamel N., Zhang Z., Wang C.M., Reddy J.N., Wang Q., Michelitsch T., Collet B., 2014, On nonconservativeness of Eringen's nonlocal elasticity in beam mechanics: correction from a discrete-based approach, *Archive of Applied Mechanics* **84**(9): 1275-1292.
[50] Hache F., 2018,*Vibration of Nonlocal Carbon Nanotubes and Graphene Nanoplates*, Université de Bretagne Sud.
[51] Bert C.W., Malik M., 1996, Differential quadrature method in computational mechanics: A review, *Applied Mechanics Reviews* **49**(1): 1-28.
[52] Malekzadeh P., Golbahar Haghighi M.R., Atashi M.M., 2010, Out-of-plane free vibration of functionally graded circular curved beams in thermal environment, *Composite Structures* **92**(2): 541-552.
[53] Zhang Y.Y., Wang C.M., Tan V.B.C., 2009, Assessment of timoshenko beam models for vibrational behavior of single-walled carbon nanotubes using molecular dynamics, *Advances in Applied Mathematics and Mechanics* **1**(1): 89-106.
[54] Arash B., Ansari R., 2010, Evaluation of nonlocal parameter in the vibrations of single-walled carbon nanotubes with initial strain, *Physica E: Low-Dimensional Systems and Nanostructures* **42**(8): 2058-2064**.**